Open access • Journal Article • DOI:10.1002/ADMA.200400599

Magnetic Nanocomposite Micelles and Vesicles — Source link

Sébastien Lecommandoux, Olivier Sandre, Frédéric Chécot, Juan Rodríguez-Hernández ...+1 more authors

Institutions: University of Bordeaux, Pierre-and-Marie-Curie University

Published on: 22 Mar 2005 - Advanced Materials (Wiley-Blackwell)

Topics: Magnetic nanoparticles, Polymersome, Ferrofluid, Vesicle and Nanocomposite

Magnetic Nano-composite Micelles and Vesicles

Sébastien Lecommandoux, Olivier Sandre, Frédéric Chécot, Juan Rodriguez-Hernandez, Régine Perzynski

To cite this version:

Sébastien Lecommandoux, Olivier Sandre, Frédéric Chécot, Juan Rodriguez-Hernandez, Régine Perzynski. Magnetic Nano-composite Micelles and Vesicles. Advanced Materials, Wiley-VCH Verlag, 2005, 17 (6), pp.712-718. 10.1002/adma.200400599 . hal-00392707v2

HAL Id: hal-00392707

https://hal.archives-ouvertes.fr/hal-00392707v2

Submitted on 22 Mar 2019

This document is the Accepted Manuscript version of a Published Work that appeared in final form in *Adv. Mat.*, 2005, Vol. 17, 712-718, after peer review and technical editing by the publisher. To access the final edited and published work see http://onlinelibrary.wiley.com/doi/10.1002/adma.200400599/abstract

Magnetic Nano-composite Micelles and Vesicles

Pr. Sébastien Lecommandoux*[1], Dr. Olivier Sandre*[2], Dr. Frédéric Chécot[1],

Dr. Juan Rodriguez-Hernandez[1], Prof. Régine Perzynski[3]

[1]Laboratoire Chimie des Polymères Organiques (LCPO), UMR 5629 CNRS-ENSCPB,
Université Bordeaux 1, 16, avenue Pey Berland, 33607 Pessac France
[2]Laboratoire Liquides Ioniques et Interfaces Chargées, UMR 7612 CNRS, Université Pierre et
Marie Curie, 4, place Jussieu – case 63, 75252 Paris cedex 05 France
[3]Laboratoire Milieux Désordonnés et Hétérogènes, UMR 7603 CNRS, Université Pierre et
Marie Curie, 4, place Jussieu – case 78, 75252 Paris cedex 05 France

*corresponding authors: Pr. Sébastien Lecommandoux, e-mail: lecommandoux@enscbp.fr;

Dr. Olivier Sandre, e-mail: osandre@enscbp.fr

Keywords: colloids, nano-composites, block copolymers, ferrofluids, self-assembly

Abstract: Novel magnetic nano-composites are obtained by the self-assembly in water of polypeptide based diblock copolymers polybutadiene-*b*-poly(glutamic acid) combined with hydrophobically modified γ-Fe_2O_3 nanoparticles. These hybrid supramolecular objects are either filled micelles (3-d) or hollow vesicles with a magnetic membrane (2-d), which deformation under an applied magnetic field has been evidenced.

Graphic for TOC:

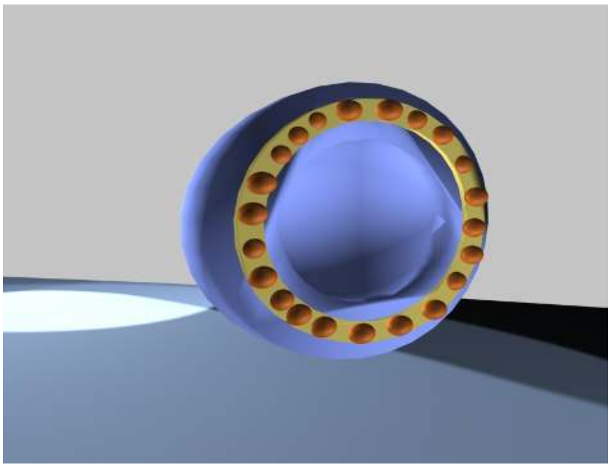

Artist view of a magnetic vesicle made of a diblock copolymer membrane confining magnetic nanoparticles. The shape is cut in half so that one sees the monolayer of nanoparticles (red) embedded in the hydrophopic blocks (yellow) of the bilayer, with its hydrophilic blocks (blue) exposed to both the outer and inner media. The interior is free for encapsulation of aqueous species.

High or low molecular weight synthetic amphiphiles of many types have been revealed as interesting building blocks that can lead to highly ordered self-assembled structures in water.[1] Depending on their molecular architecture and on external parameters such as temperature or pH, numerous morphologies have now been caught up including micelles, vesicles, tubules and more complicated morphologies reminiscent of internal compartments of biological cells.[1,2] The bilayer formation obtained by the self-assembly of certain lipids in water is certainly the most interesting morphology both for materials science and biological perspectives.[2,3] Nevertheless, applications involving these so-called *liposomes* are generally limited by their lack of stability related to the small hydrophobic layer thickness forming the core of the liposome membrane.[4] Different groups reported on the vesicle formation from block copolymers in water (called *polymersomes*) and discussed on the improvement of the mechanical properties of the membrane obtained.[5] Recently, vesicles have also been obtained from peptide-based diblock copolymers in our group[6] and are called *peptosomes*.[7]

In this context, the introduction of nanoscopic inorganic objects in self-organized structures is still a challenge for physico-chemists, even if Nature produces and uses frequently these hybrids. For example, colloidal particles of calcium carbonate or phosphate[8] or iron oxides[9] are commonly observed in organisms, where they are often confined in vesicles. In addition to the biomimetic aspect, the introduction of nanometric inorganic compounds in a self-assembled organic matrix raises the question of the resulting structure of the hybrids. Two extreme cases are possible: the inorganic nanoparticles can be either diluted and used as local probes for scattering methods, or they can really participate to the supramolecular structure and modify the resultant properties. A pioneering work on the entrapment of inorganic particles in vesicles was done by Fendler et coll.[10] Previous studies on polymers and nanoparticles have dealt with the stabilization of these colloidal particles with low or high molecular weight polymers[11] or with their introduction into macroscopic polymeric gels.[12] The topic here is somehow different, for we are interested in the inclusion of magnetic nanoparticles into supramolecular objects at the mesoscopic scale and in the study of the resulting structures and properties. Recently, such vesicles and nanocomposites of inorganic moieties and peptide-type amphiphiles have been developed respectively by Katagiri et al.,[13] Stupp et al.,[14] and Deming et al.[15]. The closest approach to ours concerns extremely well defined clusters of magnetic nanoparticles confined in micelles of diblock copolypetides,[16] except that we are looking here for larger objects exhibiting a more complex magnetic response that mere magnetization.

We report indeed on the preparation of a novel type of hybrid colloids, based on the association of several polymeric systems and ferrofluids. On the one hand, we use inorganic nanoparticles made of a magnetic iron oxide that respond to a magnetic field of low intensity. On the other hand, the organic part is made of mesoscopic structures (vesicles and micelles) self-assembled from amphiphile polybutadiene-*b*-poly(glutamic acid) diblock copolymers. Those PB-*b*-PGA copolymers bearing a *rod-coil* structure with a cross-linkable hydrophobic block and a hydrophilic peptidic block have been synthesized recently by combining anionic polymerization and ring-opening polymerization.[6] Due to a helix-coil transition of the PGA block, such peptosomes behave as stimuli-responsive nanocapsules as they respond to a pH-change by a variation of their hydrodynamic diameter as large as 50%.[6,17] As for the magnetic nanoparticles, they come from *ferrofluids* which are colloidal suspensions of nanometric magnetic grains stabilized either by electrostatic charges in aqueous media,[18] or by appropriate tensioactives in organic solvents.[19] Embedded in supra-macromolecular objects formed by diblock copolymers, these inorganic nanoparticles are used as structural probes in small angle neutron scattering (SANS) experiments. Benefiting from the strong contrast of iron oxide compared to polymer and solvent, we measure the structure factor inside the aggregates $S_{intra}(q)$. On the one hand, this curve reflects the interactions between the nanoparticles and possibly the mean inter-particle distance, hence their local concentration.[20] On the other hand, $S_{intra}(q)$ can be identified at low q to the global form factor $P_{agg}(q)$ of the object that they decorate.[21] Another guiding idea of this mineralization is to bring a magnetic response to the whole object, either an induced shape change towards an ellipsoid or a more complex shape or to trigger the delivery of an active substance by the application of a field. It has been soon predicted indeed that liposomes exhibit an ellipsoidal deformation in strong magnetic fields.[22] Depending on the sign of the magnetic susceptibility anisotropy $\Delta\chi=\chi_{\parallel}-\chi_{\perp}$ of the bilayer, the shape is either an elongated (prolate) or a flattened (oblate) ellipsoid. However, this phenomenon requires field intensities B of 1 Tesla (10^4 G) at least, due to a too small natural anisotropy $\Delta\chi<10^{-7}$ for a classical lipid (lecithin) bilayer.[23] Better magnetically alignable membranes can be obtained by adsorption of paramagnetic ions like lanthanides.[24] But theory predicts that the greatest enhancement of the magnetic response would be obtained by filling the interiors of the vesicles with magnetic nanoparticles.[25] Anisotropic SANS patterns have been reported for pure lipid vesicles in strong magnetic fields B from 1 to 4 Tesla.[26] Using the same spectrometer (PAXY, LLB, CEA-Saclay, France), we show here by SANS not only the orientation but also the *deformation* of copolymer membranes stuffed with magnetic nanoparticles.

This work starts by the verification that those organic and inorganic systems can effectively be combined together to generate well defined and properly dispersed objects. Therefore we examine a series of PB-*b*-PGA copolymers which differ by the length of their polypeptide PGA block. We present a short series of samples representative of the micellar and vesicular structures confining magnetic nanoparticles in either 3 or 2 dimensions respectively. We start from the following original structures as building bricks:

- PB_{48}-*b*-PGA_{114} and PB_{48}-*b*-PGA_{145} which self-assemble in water as micelles of hydrodynamic diameters d_H=60 nm and d_H=70 nm respectively as determined by DLS, the internal diameter of the hydrophobic core measured by SANS being d_{int}=14 nm for both.[27]

- PB_{48}-*b*-PGA_{56} which forms closed membranes in water, *i.e.* vesicles characterized by an outer diameter d_H =100 nm and a hydrophobic thickness δ_{PB}=14 nm inside the bilayer measured by SANS matching the contrast of PGA blocks.[27]

- a ferrofluid in dichloromethane denoted S2-CH_2Cl_2, consisting of maghemite nanoparticles with a characteristic diameter d_0=7.6 nm (see Supplemental Information I for the methods to measure and to decrease their polydispersity in sizes and to graft an appropriate surfactant).

Table 1: Short summary of samples and self-assembled hybrid objects that have been prepared.

PB_n-*b*-PGA_p copolymers γ-Fe_2O_3 nanoparticles	PB_{48}-*b*-PGA_{145} Micelles in water	PB_{48}-*b*-PGA_{114} Micelles in water	PB_{48}-*b*-PGA_{56} Vesicles in water
S2-CH_2Cl_2 - in dichloromethane - surfactant coating - size polydispersity: d_0=7.6nm and σ =0.25	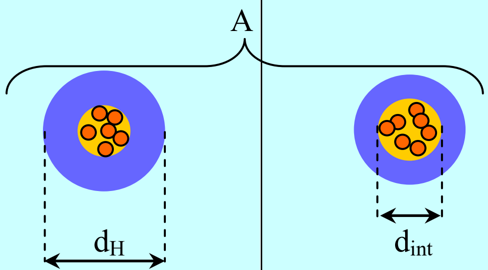 Magnetic micelles	Magnetic micelles	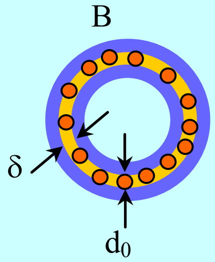 Magnetic vesicles

Table 2: Characterization of the nano-composites under study (average volume fraction of ferrofluid nanoparticles, size and shape of the aggregates).

Copolymer	Ferrofluid	Eq. ferro[a]	Solvent	System[b]	Φ_{ferro} (%)[c]	d_H (nm) [d]	R_G (nm) [e]	morphology	N_{part}[f]
PB_{48}-*b*-PGA_{145}	S2-CH_2Cl_2	1	H_2O	A	0.26	429	123	Micelles	80000
		2		A	0.043	225	95	Micelles	12000
PB_{48}-*b*-PGA_{114}	S2-CH_2Cl_2	1	H_2O	A	0.14	333	108	Micelles	38000
		2		A	0.021	260	110	Micelles	18000
PB_{48}-*b*-PGA_{56}	S2-CH_2Cl_2	1	H_2O	B	0.30	624	256	Vesicles	12000
		2		B	0.26	208	104	Vesicles	2700

[a] mass equivalent of iron oxide compared to copolymer in the preparation mixture.
[b] code corresponding of the system related to Table 1 and to the text.
[c] volume fraction of ferrofluid in the final suspension (measured by titration of iron).
[d] hydrodynamic diameter measured by multi-angle DLS with CONTIN analysis.
[e] radius of gyration measured from a Guinier fit of the low angle light scattering.
[f] approximate number of nanoparticles per object (estimated by formulae in the text).

Micelles of PB_{48}-*b*-PGA_{114} and PB_{48}-*b*-PGA_{145} mixed with surfacted ferrofluid S2-CH_2Cl_2 (A) lead to a stable (over months) dispersion of magnetic micelles in water, as attested by the structure factor deduced from SLS and SANS. Combined with 1 mass equivalent of ferrofluid, both diblock copolymers lead to fully dispersed suspensions. On the contrary at 2 mass equivalents, a *coagulum* is still present after several weeks, leading to much lower concentrations of dispersed objects (Table 2). The radii of gyration of the objects are of the order of 100 nm and smaller than (half of) the hydrodynamic diameters d_H which are ranging from 225 nm to 430 nm (Table 2). The ratios $2R_g/d_H$ between 0.6 and 0.8 are close to the hard sphere value $(3/5)^{0.5} \approx 0.77$. There is a large (several-fold) increase of the outer diameters compared to unloaded micelles (d_H=60 nm and 70 nm for pure PB_{48}-*b*-PGA_{114} and PB_{48}-*b*-PGA_{145} respectively), which means the self-assembly of the diblocks is significantly modified by the presence of the nanoparticles. The position of the structure peak around $q_{max} \approx 8\ 10^{-2}$ Å^{-1} (Figure 1) corresponds to a short inter-particle distance $d_{max} \approx 8$ nm. The hydrophobic cores are thus filled with nanoparticles at a volume fraction $\Phi_{\text{ferro}}^{\text{local}} = \frac{\pi}{6}\left(\frac{d_0}{d_{\text{max}}}\right)^3$ about 45%, of the order of the dense packing value. This high encapsulation yield together with the global 3-d shape of the aggregates are confirmed by a look at the TEM (Figure 2) and AFM images (Supplemental Information II) in the case of PB_{48}-*b*-PGA_{114}, which show large and thick baggies of inorganic particles of sizes comparable to the determinations of Table 2. The nanoparticles appear compactly confined in localized volumes. Those objects do not resemble at all to the tenuous fractal clusters observed when magnetic nanoparticles

This document is the Accepted Manuscript version of a Published Work that appeared in final form in *Adv. Mat.*, 2005, Vol. 17, 712-718, after peer review and technical editing by the publisher. To access the final edited and published work see http://onlinelibrary.wiley.com/doi/10.1002/adma.200400599/abstract

spontaneously aggregate.[28] The over-concentration in these baggies compared to the very low global concentration of nanoparticles in the suspension ($\Phi_{ferro}\approx 0.1\%$) means that the nanoparticles inside the micelles are almost in contact to each other, the remaining space inside the bags being taken by the PB blocks (about 55vol.%). In these peptide-based micellar systems, the average number of magnetic nanoparticles per micelle can be estimated by $N_{part} = \frac{\pi}{6}\left(\frac{d_H}{d_{max}}\right)^3$ (see Table 2). Each micelle contains a few 10^4 nanoparticles, which is two orders of magnitude larger than in aggregates of magnetic nanoparticles obtained by the addition of coagulating homopolymers,[29,30] or other self-assembling diblock copolymers.[16]

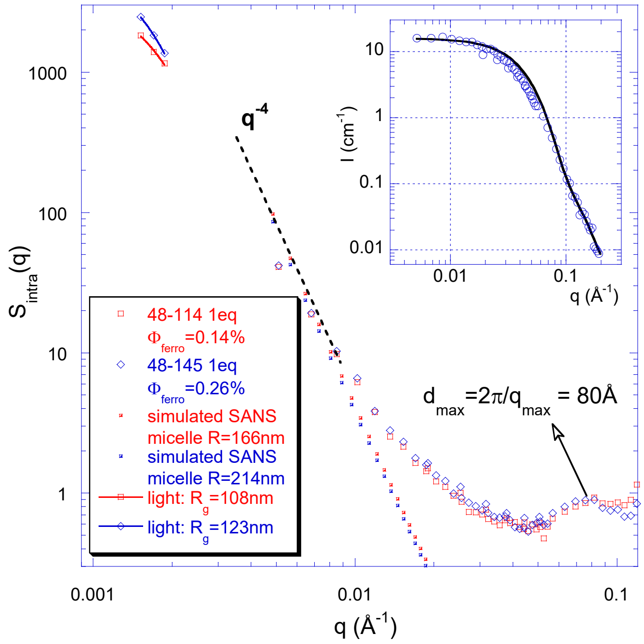

Figure 1: *Intra-aggregate structure factor $S_{intra}(q)$ of the hydrophobic nanoparticles S2-CH_2Cl_2 associated to PB_{48}-b-PGA_{114} and PB_{48}-b-PGA_{145} copolymers. The dash line corresponds to a slope q^{-4}. The square dots represent simulations of the SANS intensities for spherical micelles of the given radii. The few points at lowest q come from SLS and enable an estimate of the radii of gyration by a standard Guinier fit. The inset shows the SANS curve of the dilute ferrofluid fitted by the form factor $P_{ferro}(q)$ of polydisperse spheres* (d_0=7.6 nm and σ=0.25).

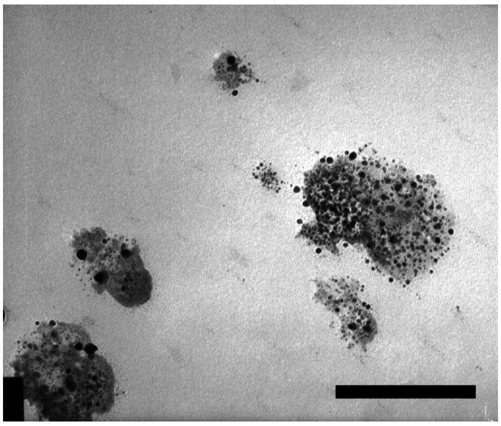

Figure 2: *TEM picture of hybrid copolymer micelles loaded with magnetic nanoparticles obtained by combining PB_{48}-b-PGA_{114} and 1 mass equiv. of surfacted ferrofluid S2-CH_2Cl_2. The scale bar measures 400 nm.*

Vesicles of PB_{48}-*b*-PGA_{56} still form in water even in the presence of S2-CH_2Cl_2 (B), as attest the structure factors deduced from SLS and SANS (Figure 3). Their outer diameter is significantly increased by the presence of the nanoparticles (d_H equal to 620 nm and 210 nm for 1 and 2 mass equivalents respectively). The ratios $2R_g/d_H$ of the radii of gyration (Table 2) over half of the hydrodynamic diameters are close to 1, the theoretical value for a hollow sphere. Due to their hydrophobic coating, the nanoparticles are confined in 2-d between the two leaflets of the copolymer bilayer, as proved together by SANS measurements, TEM pictures and AFM imaging (which in addition contains a valuable topographical information). Figure 3 represents the intra-aggregate structure factor $S_{intra}(q)$ measured by SANS for the hydrophobic nanoparticles associated to PB_{48}-*b*-PGA_{56} diblock copolymer forming vesicles. In the small q-regime, $S_{intra}(q)$ is identical to the form factor of the aggregate $P_{agg}(q)$ and follows a power law with a slope approximately q^{-2}, completely different from the q^{-4} slope of Figure 1. This q^{-2} slope could be associated to 3-d aggregation of the nanoparticles under Diffusion or Reaction Limited Aggregation processes (DLA or RLA). However, both TEM pictures of Figure 4 and AFM measurements (which are discussed in Supplemental Information II) do not correspond to such a fractal cluster formation. On the contrary, one can calculate the thickness δ of the layer forming the vesicle membrane from the asymptotic Kratky-Porod approximation in this q-region for the form factor of a flat infinite sheet of thickness δ:[31] $\mathrm{Ln}[S_{intra}(q)*q^2]\approx \mathrm{Ln}(I_0)-q^2\delta^2/12$, where I_0 is proportional to the surface area. We get δ_{1eq}=8.6 nm and δ_{2eq}=17.7 nm respectively for the system with 1 equivalent and 2 equivalents of ferrofluid. Note that here the SANS contrast is given by the nanoparticles only and that δ is an inorganic thickness which do not take into account the copolymer. As the typical diameter d_0 of the nanoparticles is 7.6 nm, one can conclude that this membrane contains either one or two layers of the magnetic colloids depending on the equivalent ratio at preparation. Instead of the Kratky-Porod approximation, one can also simulate the form factor of vesicles with radius R (taken as $d_H/2$) and membrane thickness δ. The good adjustment of the curves confirms unambiguously the presence of flat sheets of thickness δ, but their radius of curvature R cannot be measured precisely in this q-range. At wider angle, the scattered intensities are dominated by the magnetic nanoparticles and thus $S_{intra}(q)$ reaches 1. The absence of correlation distance $d_{max}=2\pi/q_{max}(=8nm)$ between neighboring nanoparticles for the preparation at 1 equivalent of ferrofluid corroborates the fact that the inorganic colloids form at most one monolayer inside the polymeric membrane. Assuming a close-packing of the nanoparticles within the shell, one estimates the maximum number of nanoparticles per vesicle (see Table 2) as $N_{part} \approx \frac{\pi}{\sqrt{3}} n_{layers} \left(\frac{d_H}{d_0}\right)^2$ where n_{layers} is the number of layers, identical to the number of equivalents (1 or 2). The bidimensional character of the objects is also visualized directly by TEM (Figure 4) and AFM (Supplemental Information II). Those patterns look neither like spontaneously aggregated nanoparticles[28] nor to clusters induced by other (co)polymers.[16,29,30]

This document is the Accepted Manuscript version of a Published Work that appeared in final form in *Adv. Mat.*, 2005, Vol. 17, 712-718, after peer review and technical editing by the publisher. To access the final edited and published work see http://onlinelibrary.wiley.com/doi/10.1002/adma.200400599/abstract

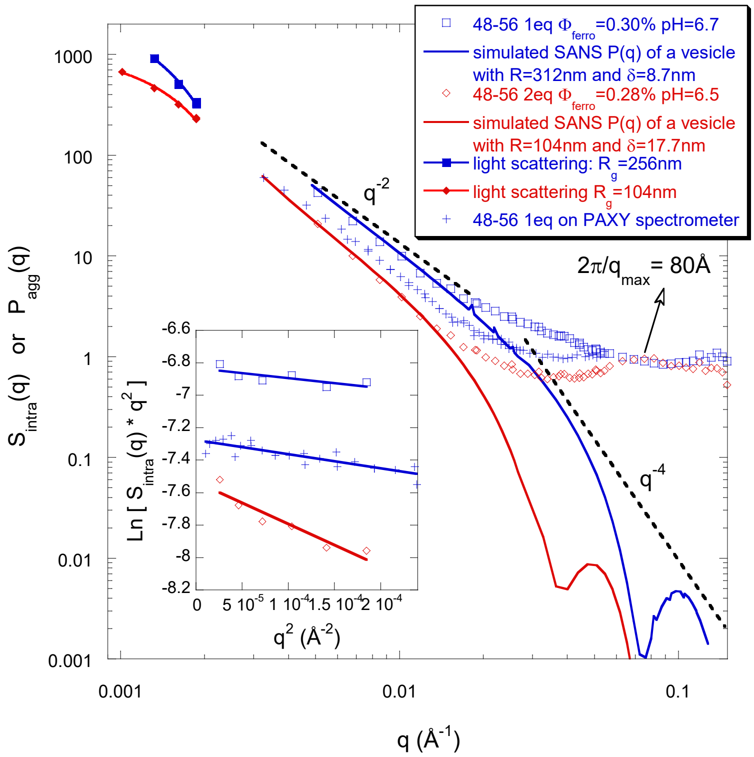

Figure 3: SANS measurements of the intra-aggregate structure factor $S_{intra}(q)$ of hydrophobic nanoparticles S2-CH_2Cl_2 (1eq and 2eq) associated to PB_{48}-b-PGA_{56}. The solid lines represent simulations of the SANS intensities in the same conditions as the experiments for hollow vesicles with following dimensions: R_{1eq}=312 nm and δ_{1eq}=8.7 nm, R_{2eq}=104 nm and δ_{2eq} =17.7 nm, respectively. Data for 1eq obtained in light water by full angular averaging of the 2-d PAXY spectrometer under zero field are added to show $S_{intra}(q)$ at lower q (the overlap with data acquired on PACE is not perfect as the solvent is not contrast matched to polymer in that case). They lead however to the same q^{-2} behavior. The few points at lowest q come from static light scattering and give estimates of the radii of gyration from a Guinier fit. The inset shows Kratky-Porod plots, which slope give the values δ_{1eq} and δ_{2eq} of membrane thickness given above. A thickness δ_{PAXY}=10 nm somehow larger than δ_{1eq} is found from the data measured on PAXY, presumably due to the contribution of the copolymer to the neutron scattering contrast.

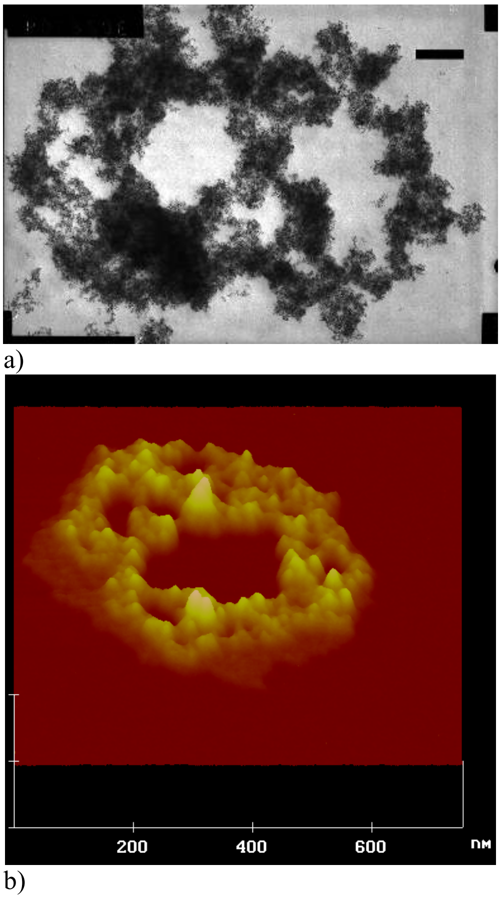

Figure 4: a) TEM picture of a magnetic membrane made of PB_{48}-b-PGA_{56} and 1 equiv. of S2-CH_2Cl_2. The scale bar measures 333 nm. b) 3-d view built from an AFM picture of the same sample (see Supplemental Information II) showing a flat copolymer membrane stuffed with magnetic iron oxide nanoparticles. Strong spreading on mica opens holes in the central part, whereas some pure copolymer bilayer is visible at the periphery.

The magnetic response of vesicles of PB_{48}-*b*-PGA_{56} with the membrane filled with 1eq S2-CH_2Cl_2 (B) is studied using anisotropic SANS under an applied magnetic field. The system is dispersed in light water (H_2O) to work in (almost) pure nuclear contrast under field.[32] The scattering patterns become clearly anisotropic when a magnetic field is applied to this sample (Figure 5a). The iso-intensity curves in the 3 10^{-3}–2 10^{-2} Å^{-1} q-range are ellipses elongated perpendicularly to the field direction, with aspect ratios increasing from 1.1 to 1.3 when the field intensity B increases from 290 to 1450 G, almost independently of the value of q. The scattering patterns are also analyzed at a constant q, as a function of the angle θ with the field direction. The intensity profile $I_{B=1050G}(\theta)$ normalized by the isotropic intensity $I_{B=0}(\theta)$ is plotted in Figure 5b for several values of q between 4 10^{-3} Å^{-1} and 9 10^{-3} Å^{-1}. The ratio is maximum in the direction perpendicular to the field ($I_\perp/I_{B=0}$=1.1–1.15) and minimum in the direction parallel to the field ($I_{||}/I_{B=0}$=0.6–0.7). We deduce an anisotropy parameter ($I_\perp$-$I_{||}$)/$I_{B=0}$≈0.5 for this field value B=1050 G.

However, it would be a mistake to consider that such a ratio measured on the scattering patterns represents directly the shape anisotropy of the vesicles under a magnetic field. One has indeed to remember that the window 3 10^{-3}–5 10^{-2} Å^{-1} of scattering vectors q explored by these SANS measurements under field lies far above the Guinier regime, which is in the domain of small angle light scattering. Instead of the global shape of the vesicles, these experiments tell us about the deformation at the length scale of the membrane thickness δ. Besides, we checked that this anisotropy under field does not originate from magnetic dipolar interactions between nanoparticles.[32,33] The nuclear SANS pattern under field of the same ferrofluid at high concentration in water exhibits no anisotropy at all indeed. An anisotropy due to magnetic scattering being also excluded in light water,[32] we deduce that the anisotropy of the SANS patterns described here reflects a *sensitivity to the magnetic field of the spatial distribution of the nanoparticles within the membranes.* An exhaustive analysis of the field-induced anisotropy in the two principal directions || and ⊥ relatively to the magnetic field is presented in Supplemental Information III. It shows that either the membrane becomes stretched in the portions of shell crossed by the magnetic field (decrease of the apparent membrane thickness $\delta_{||}$), or almost equivalently that the magnetic nanoparticles move away from the magnetic poles. The remaining parts of the membrane remain unaffected ($\delta_{\perp}$ almost equal to the initial bilayer thickness at B=0 G). Until now, the deformation under field of hollow objects with a magnetic material confined in 2 dimensions has only been examined theoretically.[34,35] Even though more investigations with high resolution microscopy like cryo-TEM could help by directly imaging those vesicles "frozen" under field, the anisotropic SANS presented here already provides an unambiguous evidence of their shape sensitivity to the magnetic field. To the authors' knowledge, this is the first described example of vesicles with a *deformable magnetic* membrane. Other magnetic shells have been indeed mentioned in literature,[36,37] but none as thin and floppy as these.

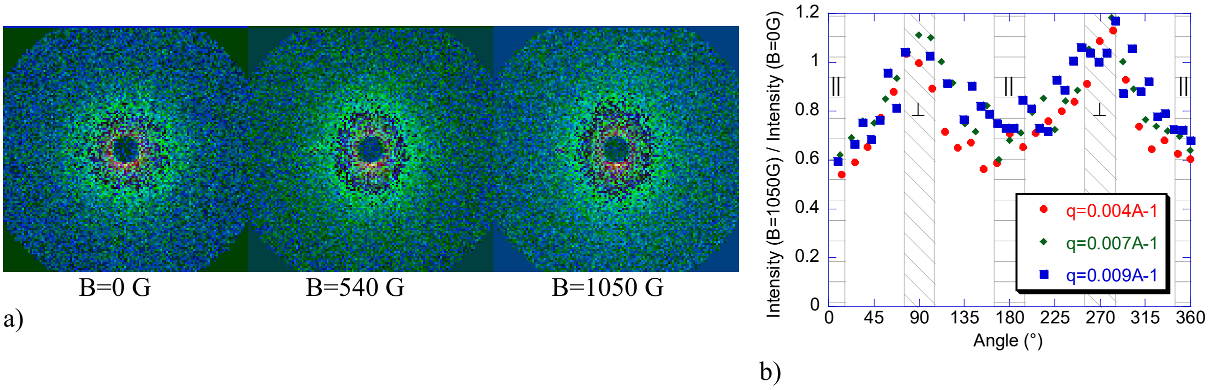

Figure 5: Deformation of hollow magnetic shells (system B 1eq) studied by anisotropic SANS.

a) 2-dimensional SANS patterns under a magnetic field (directed horizontally). The anisotropy is observed in the q range 3 10^{-3}*–2* 10^{-2} Å^{-1}*. b) Intensity profile for B=1050 G normalized by the intensity for B=0 G vs. angle* θ *with the field direction for several values of q. The dashed intervals correspond to the angular regroupings respectively || and ⊥(see Supplemental Information III).*

Conclusions

To summarize, the main challenge addressed in this paper is to build supra-macromolecular objects from magnetic nanoparticles and diblock copolymers. At first, the nanoparticles are used as structural probes to elucidate the transformation of the micelles and vesicles by the insertion of the inorganic material itself. Spherical micelles in water (samples A) are filled with a hydrophobic ferrofluid at volume fraction as high as 45%. With the same nanoparticles and another length of the PGA blocks of the copolymers, hollow fluid magnetic spheres are obtained (samples B). The organic amphiphile copolymers confine the inorganic nanoparticles coated by surfactants within the thin layer of PB blocks. Furthermore, anisotropic SANS data bring the experimental evidence of the capability to modify the shape of these mineralized membranes in response to a magnetic field of intensity as low as B=290 G.

At last, one can imagine potentialities of these superparamagnetic micelles and vesicles in biomedicine and biotechnology, related the specific properties of magnetic iron oxide: manipulation by an external magnetic field gradient, radio-frequency heating for cancer therapy,[38] labeling of organs in Magnetic Resonant Imaging.[39] Due to their small dimensions, these objects are potential candidates for intravenous injection. The possible toxicity for cells to contact iron oxide directly would not be an issue because it is embedded in copolymer. The soft magnetic shells are especially promising for drug delivery, their internal compartment being available for encapsulation of water soluble species. A pH change or the application a magnetic field could trigger the transient opening of the bilayer and the release of an encapsulated content.

Experimental

The copolymer – nanoparticles self-assemblies were prepared by mixing 20 mg of each copolymer with either 1 or 2 mass equivalents of surfacted ferrofluid S2-CH_2Cl_2 (Table 1). The mixture was stirred for 2 h in the open air to eliminate dichloromethane. The resulting pellet was slowly redispersed in 2 mL of aqueous solvent. Addition of 50 μL of NaOH 2 mol/L enabled to deprotonate ≈75 mol% of the acidic groups of the copolymer, raising pH up to ≈7. After three weeks of vigorous stirring at T=37°C, all suspensions were analyzed by static and dynamic light scattering (SLS and DLS) and small angle neutrons scattering (SANS). Thus we could check the dispersion state and study the equilibrium shapes and sizes.

The isotropic SANS experiments were performed on the PACE spectrometer of the Laboratoire Léon Brillouin (CEA-Saclay, France). We used two configurations with sample-to-detector distance D=4.75m and two neutrons wavelengths λ=17 Å and λ=8 Å to cover q-ranges $5\ 10^{-3}$–$5\ 10^{-2}$ Å^{-1} and $2\ 10^{-2}$–$2\ 10^{-1}$ Å^{-1} respectively. The calculated contrast of neutrons scattering length densities is $\Delta\rho=5.0\times10^{10}$ cm^{-2} between γ-Fe_2O_3 and the solvent matching the copolymers, which is a 36:64 w/w mixture of D_2O and H_2O. The scattered intensity curves of the samples held in 1 mm quartz cells were corrected from incoherent background and normalized by the signal of water. Following a method used for other kinds of colloids – micelles nano-composites,[21] the intensity curves of the copolymer – nanoparticles complexes were divided by the volume fractions Φ_{ferro} and by the form factor $P_{ferro}(q)$ of the nanoparticles measured independently (see inset of Figure 1). This procedure yields the intra-aggregate structure factor $S_{intra}(q)$ of the nanoparticles associated to the block copolymers. The form factors of hollow vesicles taking into account the polydispersity of radii and the experimental resolution of PACE were calculated with a program written by Dr. J. Oberdisse.[21]

The anisotropic SANS experiments were performed on the PAXY spectrometer of the Laboratoire Léon Brillouin (CEA-Saclay, France) equipped with a 2-d detector made of 128 x 128 cells. The sample was placed between the poles of an electromagnet producing a homogeneous magnetic field, which intensity was measured with a Gaussmeter (Walker Scientific, Worcester, MA). We used two configurations with sample-to-detector distance D=6.775m and two neutrons wavelengths λ=12 Å and λ=6 Å to cover q-ranges 3 10^{-3}–3 10^{-2} $Å^{-1}$ and 7 10^{-3}–5 10^{-2} $Å^{-1}$ respectively. Due to complete isotopic exchange with atmosphere, the solvent of this PB_{48}-*b*-PGA_{56} / 1eq S2-CH_2Cl_2 sample under magnetic field was pure H_2O, thus not matching the contrast of the copolymer, but insuring a negligible magnetic scattering of iron oxide.[32] Nevertheless, the nuclear contrast of the nanoparticles $\Delta\rho=7.5\times10^{10}$ cm^{-2} was still three times larger than the contrast of the copolymer $\Delta\rho=2.5\times10^{10}$ cm^{-2}. A full angular averaging of the cells at constant q was realized for the isotropic scattering patterns. An anisotropic analysis was applied to the scattering patterns under magnetic field. By masking the appropriate cells of the 2-d detector, the intensity was averaged in angular sectors either (-15°,15°) along the field direction and thus called $I_{||}(q)$, or (75°,105°) around the perpendicular direction and denoted $I_{\perp}(q)$.

Static and dynamic light scattering was performed on a Macrotron spectrometer (Amtec, France) equipped with a He/Ne laser and a Malvern 7132 correlator. Aliquots of the samples (1 mL in cylindrical vials) diluted 20–100 times in 0.2 µm filtered water were immersed in a filtered toluene bath with temperature regulated at 25°C. For DLS, the autocorrelation functions of the intensity scattered at various angles from 45° up to 155° every 5° were recorded using a 0.5 µs sampling time for a duration of 15 min per angle. Using the standard program CONTIN, the dominant decay rate Γ_{max} was extracted and plotted *vs.* q^2 to get the hydrodynamic diameters d_H from the slope extrapolated in the low-q limit. For SLS, the light intensity was time-averaged and corrected from geometrical and polarization effects so that the signal of filtered toluene appears independent of the angle.

The molar content of iron [Fe] (mol/L) was titrated by atomic absorption spectroscopy with a Perkin Elmer Analyst 100 apparatus after degrading the nanoparticles within the nano-composites in boiling HCl (35%). The volume fraction of iron oxide was deduced from formula weight and mass density of γ-Fe_2O_3 as: Φ_{ferro}(vol%)=1.577*[Fe].

TEM pictures were recorded on a JEOL JEM100S microscope working at 100 kV. Samples were prepared by spraying a 1 $g.L^{-1}$ solution of the block copolymer associated to ferrofluid onto a TEM grid using a homemade tool.

AFM pictures of dilute samples deposited on mica (5 µL at 0.1 $g.L^{-1}$) were obtained with a Nanoscope III multimode scanning probe microscope (Digital Instruments, Santa Barbara, CA) in the Tapping Mode in air at a 512*512 pixels resolution and a 0.9 Hz scan rate.

Acknowledgements

The authors thank Pr. Harm-Anton Klok from EPFL for his help with the synthesis of the diblock copolymers, Dr. Fabrice Cousin and Dr. Julian Oberdisse as our local contacts at the LLB facilities, in particular Dr. Oberdisse for providing his program for the simulation of the form factors. Authors also acknowledge Dr. Yves Gnanou, Dr. Redouane Borsali and Pr. Valérie Cabuil for their interest and support in that work.

References:

[1] G. Riess, *Prog. Polym. Sci.* **2003**, *28*, 1107.

[2] For a review on polymer vesicles, see D.E. Discher, A. Eisenberg, *Science* **2002**, *297*, 967.

---

[3] R. Lipowsky, E. Sackmann, in *Structure and Dynamics of Membranes*, ELSEVIER, New York **1995**.

[4] a) D.D. Lasic, D. Papahadjopoulos, in *Medical Applications of Liposomes*, ELSEVIER, New York **1998**. b) D. Marsh, in *CRC Handbook of Lipid Bilayers*, CRC PRESS, Boca Raton, FL **1990**.

[5] a) J. J. L. M. Cornelissen, M. Fischer, N. A. J. M. Sommerdijk, R. J. M. Nolte, *Science* **1998**, *280*, 1427. b) B. M. Discher, Y.-Y. Won, D. S. Ege, J. C.-M. Lee, F. S. Bates, D. E. Discher, D. A. Hammer, *Science* **1999**, *284*, 1143. c) H. Aranda-Espinoza, H. Bermudez, F. S. Bates, D. E. Discher, *Phys. Rev. Lett.* **2001**, *87*, 208301. d) J. C.-M. Lee, M. Santore, F. S. Bates, D. E. Discher, *Macromolecules* **2002**, *35*, 323. e) R. Dimova, U. Seifert, B. Pouligny, S. Forster, H.-G. Döbereiner, *Eur. Phys. J.* E **2002**, *7*, 241. f) H. Bermudez, A. K. Brannan, D. A. Hammer, F. S. Bates, D. E. Discher, *Macromolecules* **2002**, *35*, 8203. g) H. Bermudez, D. A. Hammer, D. E. Discher, *Langmuir* **2004** *20*, 540.

[6] F. Chécot, S. Lecommandoux, Y. Gnanou, H.-A. Klok, *Angew. Chem. Int. Ed.* **2002**, *41*, 1340.

[7] a) S. Kimura, D. H. Kim, J. Sugiyama, Y. Imanishi, *Langmuir* **1999**, *15*, 4461. b) H. Kukula, H. Schlaad, M. Antonietti, S. Forster, *J. Am. Chem. Soc.* **2002**, *124*, 1658.

[8] S. Mann, *Angew. Chem. Int. Ed.* **2000** *39*, 3393.

[9] N. D. Chasteen, P. M. Harrison *J. Struct. Biol.* **1999**, *126*, 182.

[10] P. Herve, F. Nome, and J. H. Fendler*, J. Am. Chem. Soc.* **1984**, *106*, 8291.

[11] a) O. Spalla, B. Cabane *Colloid Polym. Sci.* **1993**, *271*, 357. b) O. Spalla *Curr. Op. Colloid & Inter. Sci.* **2002**, *7*, 179.

[12] a) J.-C. Bacri, D. Gorse, *J. Phys.* (Paris) **1983**, *44*, 985. b) M. Zrínyi, L. Barsi, A. Büki *Polymer Gels and Networks* **1997**, *5*, 415. c) C. Mayer, V. Cabuil, T. Lalot, R. Thouvenot, *Adv. Mater.* **2000**, *12*, 417. d) J. A. Galicia, O. Sandre, F. Cousin, D. Guemghar, C. Ménager, V. Cabuil, *J. Phys.: Condens. Matter* **2003**, *15*, S1379.

[13] a) K. Katagiri, R. Hamasaki, K. Ariga, J. Kikuchi, *J. Am. Chem. Soc.* **2002**, *124*, 7892. b) K. Katagiri, K. Ariga, J. Kikuchi, *Chem. Lett.* **1999**, 661.

[14] J. D. Hartgerink, E. Beniash, S. I. Stupp, *Science* **2001**, *294*, 1684.

[15] J. N. Cha, G. D. Stucky, D. E. Morse, T. J. Deming, *Nature* **2000**, *403*, 289.

[16] L. E. Euliss, S. G. Grancharov, S. O' Brien, T. J. Deming, G. D. Stucky, C. B. Murray, G. A. Held, *Nano Lett.* **2003**, *3*,1489.

---

[17] F. Chécot, S. Lecommandoux, H.-A. Klok, Y. Gnanou, *Eur. Phys. J.* E **2003**, *10*, 25.

[18] a) R. Massart, *C. R. Acad. Sci.* (Paris) Ser. C **1980** *291*, 1. b) R. Massart *IEEE Trans. Magn.* **1981**, *17*, 1247.

[19] S. Lefebure, E. Dubois, V. Cabuil, S. Neveu, R. Massart, *J. Mater. Res.* **1998**, *13*, 2975.

[20] E. Dubois, F. Boué, V. Cabuil, R. Perzynski, *J. Chem. Phys.* **1999** *111*, 7147.

[21] a) J. Oberdisse, B. Demé, *Macromolecules* **2002** *35*, 4397. b) G. Despert, J. Oberdisse, *Langmuir* **2003**, *19*, 7604.

[22] W. Helfrich, *Phys. Lett.* **1973**, *43A*, 409.

[23] G. Maret, K. Dransfeld in *Topics in Applied Physics: Strong and Ultrastrong Magnetic Fields and Their Applications,* Vol. 57 (Ed: F. Herlach), SPRINGER-VERLAG, Berlin **1985**, Ch. 4.

[24] R. S. Prosser, S. A. Hunt, J. A. DiNatale, R.R. Vold, *J. Am. Chem. Soc.* **1996**, *118*, 269.

[25] L. Auvray, *C. R. Acad. Sci.* Paris **1981**, *292*, 821.

[26] M. A. Kiselev, M. Janich, P. Lesieur, A. Hoell, J. Oberdisse, G. Pepy, A. M. Kisselev, I. V. Gapienko, T. Gutberlet, V. L. Aksenov, *Appl. Phys.* A [Suppl] **2002**, *74*, S1239.

[27] F. Chécot, *PhD thesis* **2003**, University Bordeaux 1.

[28] K. Butter, P. H. Bommans, P. M. Frederiks, G. J. Vroege, A. P. Philipse, *Nature Mat.* **2003**, *2*, 88.

[29] S. Veintemillas-Verdaguer, M. P. Morales, O. Bomati-Miguel, C. Bautista, X. Zhao, P. Bonville, R. Pérez de Alejo, J Ruiz-Cabello, M. Santos, F. J. Tendillo-Cortijo, J. Ferreirós, *J. Phys.* D: App. Phys. **2004**, *37*, 2054.

[30] D. El kharrat, O. Sandre, P. Licinio, R. Perzynski, *AIP Conf. Proc.* **2004**, *708*, 122.

[31] O. Glatter, O. Kratky, in *Small Angle X-Ray Scattering,* ACADEMIC PRESS, New York **1983**.

[32] F. Gazeau, F. Boué, E. Dubois, R. Perzynski, *J. Phys. Cond. Mater.* **2003**, *15*, S1305.

[33] F. Gazeau, E. Dubois, J.-C. Bacri, F. Boué, A. Cebers, R. Perzynski, *Phys. Rev.* E **2002**, *65*, 031403.

[34] N. Kern, B. Fourcade, *Europhys. Lett.* **1997**, *38*, 395.

[35] Y. L. Raikher, O. V. Stolbov, *J. Magn. Magn. Mater.*, in press.

[36] E. L. Bizdoacaa, M. Spasovaa, M. Farlea, M. Hilgendorff., F., Caruso*, J. Magn. Magn. Mater.* **2002** *240*, 44.

---

[37] D. G. Shchuki, G. B. Sukhorukov, H. Möhwald, *Angew. Chem. Int. Ed.* **2003**, *42*, 4472.

[38] J. Roger, J. N. Pons, R. Massart, A. Halbreich, J.-C. Bacri, *Eur. Phys. J. Appl. Phys.* **1999**, *5*, 321.

[39] C. Billotey, C. Wilhelm, M. Devaud, J.-C. Bacri, J. Bittoun, F. Gazeau, *Magn. Reson. Med.* **2003**, *49*, 646.